

34 are Rock Mass Rating (RMR) (Bieniawski 1976, 1989), Slope Mass Rating (SMR) (Romana
35 1993), Rock Mass Strength (RMS) (Romana 1985), Slope Rock Mass Rating (SRMR)
36 (Robertson 1988), Slope Stability Probability Classification (SSPC) (Hack et al. 1998),
37 Modified Stability Probability Classification (SSPC modified) (Lindsay et al. 2001), Natural
38 Slope Methodology (NSM) (Shuk 1994) and Q-slope Method (Barton and Bar 2015; Bar and
39 Barton 2017). Among all, Slope Mass Rating (SMR), calculated on the base of Rock Mass
40 Rating (RMR), is probably one of the most widely used classifications (Romana et al. 2015).
41 Many technical and educational books of rock mechanics or rock slope stability include a
42 specific chapter or section for this classification (e.g. Hudson and Harrison (1997); Singh and
43 Göel (1999)). SMR has also been included in technical regulations of some countries such as
44 Italy, USA, China and India (Romana et al. 2015; Tomás et al. 2016).

45 The assessment of the basic RMR is made by rating five parameters: 1) rock strength,
46 2) rock quality, 3) spacing, 4) condition of discontinuities, and 5) groundwater conditions.
47 Once the basic RMR has been calculated, four new factors have to be taken into account to
48 calculate the SMR index. These new factors depend on the method of excavation of the slope
49 and the relative orientation between discontinuities and slope. SMR value varies between 0
50 and 100, being 0 a completely unstable slope and 100 a completely stable one. It is important
51 to note that other values are mathematically possible, although those values higher than 100 or
52 lower than 0 do not have a physical sense.

53 Despite the apparent simplicity of this classification, often some mistakes are made
54 when it is used for professional and scientific purposes. Nearly all these mistakes involve the
55 influence of slope geometry and the strike and dip of the discontinuities. As a consequence of
56 these mistakes, the final result of the slope stability assessment can be completely inaccurate.
57 In this sense, Zheng et al. (2016) observed some problems assessing the two adjustment
58 parameter F_1 and F_3 , considering that the original SMR system may contain theory defects.
59 But actually, it is a clarification of the SMR parameters what is needed. This clarification is
60 presented in this paper through a comprehensive review of the SMR index (section 2). In
61 section 3, a complete and detailed definition of the angular relationships between
62 discontinuities and slope, and a redefinition of the mathematical equations for all the possible
63 cases are included. Additionally, to avoid potential misunderstandings, a new Matlab-based
64 open-source software has been developed in order to overcome the difficulties in the SMR
65 calculation (section 4). The performance, benefits and usefulness of SMRTool are also

66 illustrated and discussed in this paper throughout a specific case study in section 5. Finally,
67 the main conclusions are presented in section 6.

68

69 **2. SLOPE MASS RATING**

70 Rock Mass Rating (RMR) system was originally published by Bieniawski in 1976
71 (Bieniawski 1976). Since then, the RMR classification system has experienced successively
72 changes in the ratings assigned to different parameters as more case reports were studied
73 (Bieniawski 1989). Five parameters are used to classify a rock mass using the RMR
74 classification: uniaxial compressive strength of rock, Rock Quality Designation (RQD),
75 spacing of discontinuities, condition of discontinuities (further subdivided into persistence,
76 separation, smoothness, infilling and weathering) and groundwater conditions. The value of
77 RMR is equal to the sum of all these five parameters and it ranges from 0 to 100.

78 SMR index is obtained from basic RMR according to equation (1), taking into account
79 four new parameters (F_1 , F_2 , F_3 and F_4) that consider the probability of failure of the slope
80 depending on the slope method of excavation and the relative orientation between the
81 discontinuities and the slope. It is worth noting that the parameters F_1 , F_2 and F_3 depend on
82 the expected type of failure for the slope under consideration (Fig. 1).

83

$$84 \quad \quad \quad SMR = RMR + (F_1 \cdot F_2 \cdot F_3) + F_4 \quad (1)$$

85

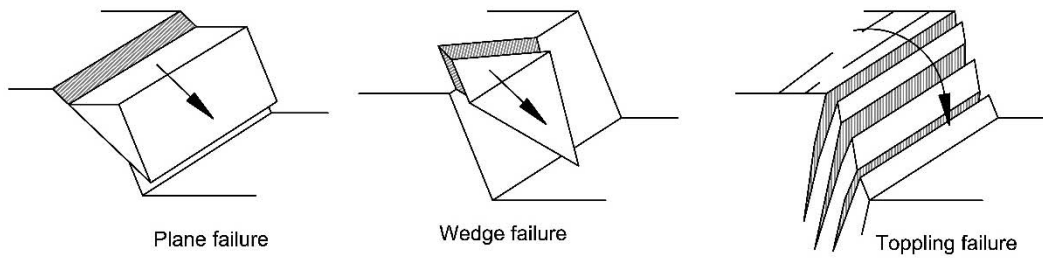
86 where

87 F_1 depends on the angle A (Fig. 2 to Fig. 4 and Table 1) between the
88 discontinuity dip direction and slope dip direction (i.e. the parallelism between: a)
89 the strikes of the discontinuity and the slope for planar and toppling failures; and b)
90 the azimuth of the line of intersection and the dip direction of the slope for wedge
91 failure).

92 F_2 depends on the discontinuity dip angle (B) (Fig. 2 to Fig. 4 and Table 1

93 F_3 depends on (Fig. 2 to Fig. 4 and Table 1): a) the difference (C) between the
94 discontinuity and the slope dip angles for plane failure; b) the sum (C) of the
95 discontinuity and the slope dip angles for toppling; or c) the difference (C) between
96 the plunge of the line of intersection and the slope dip angle for wedge failure.

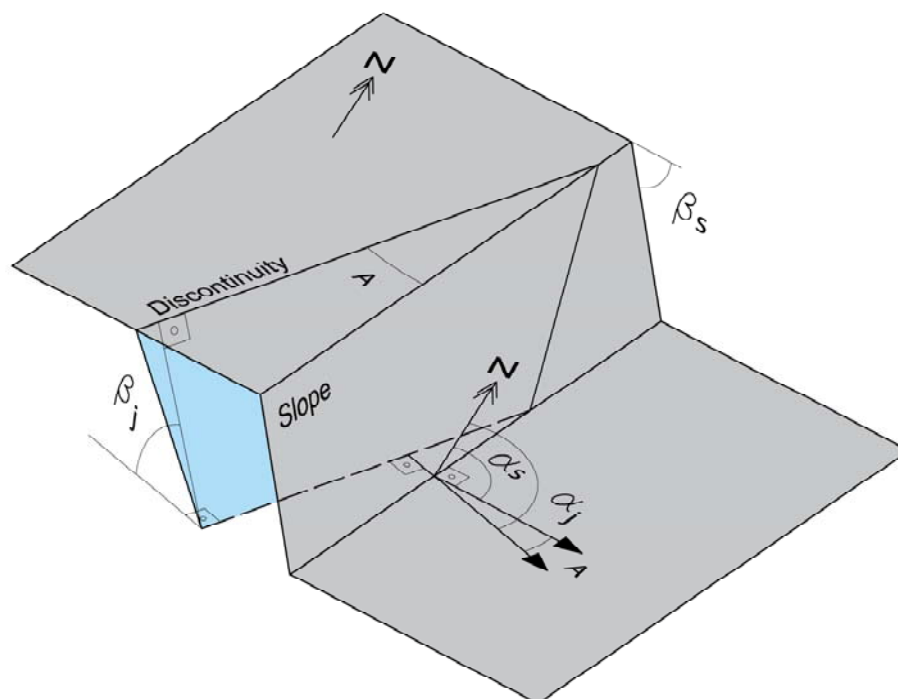
97 F_4 depends on the excavation method (Table 1).



98

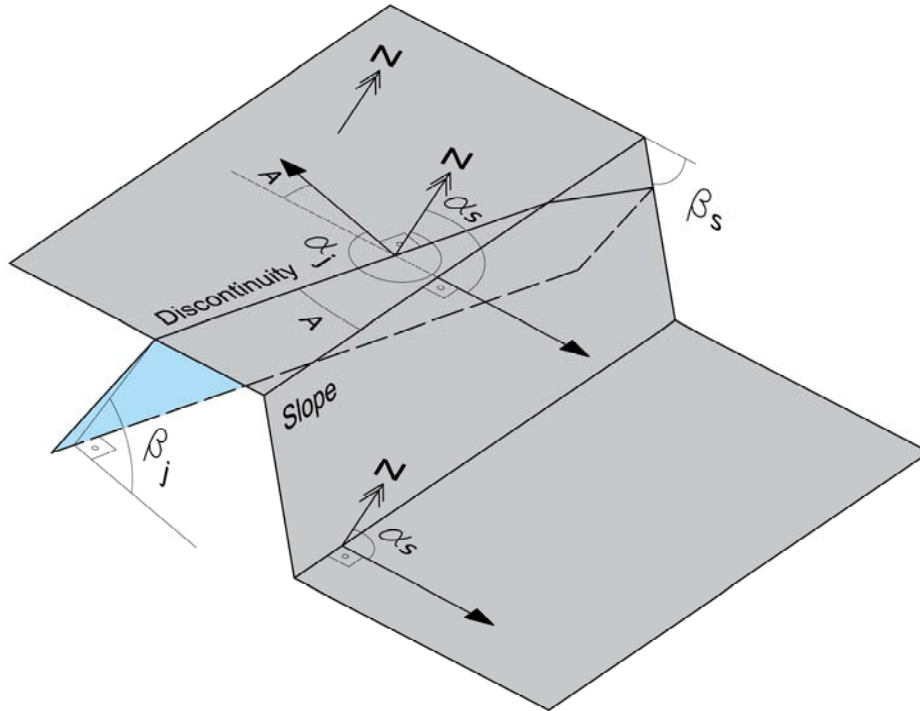
99 Fig. 1 – Types of possible slope failure to be considered in SMR calculation (Hoek and Bray
100 1981).

101



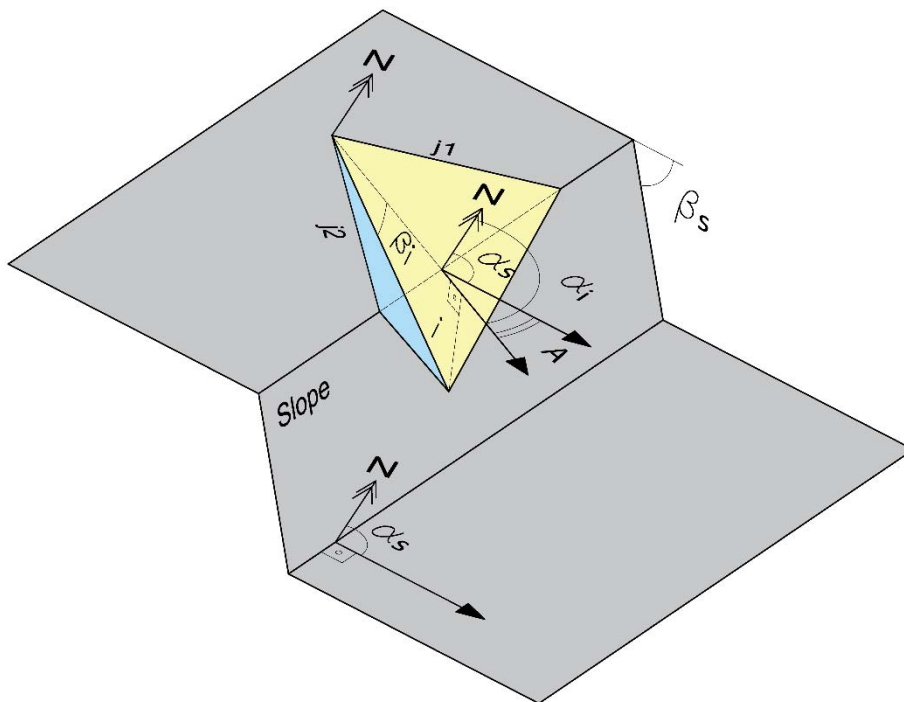
102

103 Fig. 2 – Parallelism (A) between discontinuity (α_j) and slope (α_s) strikes for planar failure.



104
105
106

Fig. 3 – Parallelism (A) between discontinuity (α_j) and slope (α_s) strikes for toppling failure.



107
108
109
110

Fig. 4 – Parallelism (A) between the plunge direction of the line of intersection of two discontinuities (α_i) and the slope dip direction (α_s).

111 The rating of these four parameters for the SMR calculation is shown in Table 1, in
 112 which it can be seen that orientation-dependent factors are zero or negative, while the
 113 excavation method factor can be positive or negative.

114

115 Table 1. Adjusting factors for discontinuities (F_1 , F_2 , and F_3) and excavation method
 116 (F_4). Modified from Romana (1985) by Tomás et al. (2007).

| Auxiliary angle Adjusting factor | Very favourable | Favourable | Fair | Unfavourable | Very unfavourable |
|-------------------------------------|--------------------|--------------|--------------------|---------------------------|-----------------------|
| A | > 30° | 30° - 20° | 20° - 10° | 10° - 5° | < 5° |
| F_1 | 0.15 | 0.40 | 0.70 | 0.85 | 1.00 |
| B | < 20° | 20° - 30° | 30° - 35° | 35° - 45° | > 45° |
| F_2 | 0.15 | 0.40 | 0.70 | 0.85 | 1.00 |
| | 1.00 | | | | |
| C | > 10° | 10° - 0° | 0° | 0° - (-10°) | < (-10°) |
| | < 110° | 110 - 120° | > 120° | - | - |
| F_3 | 0 | -6 | -25 | -50 | -60 |
| Excavation method | Natural slope | Presplitting | Smooth blasting | Blasting or mechanical | Deficient blasting |
| F_4 | +15 | +10 | +8 | 0 | -8 |

117

118 In order to make computation simpler, Romana (1993) proposed the following
 119 continuous function for F_1 and F_2 as alternative values to that shown in Table 1:

120

$$121 \quad F_1 = (1 - \sin |A|)^2 \quad (2)$$

$$122 \quad F_2 = \tan^2 B \quad (3)$$

123

124 In order to reduce subjective interpretations in the assignation of the values near the
 125 borders of the intervals, Tomás et al. (2007) proposed asymptotical continuous functions for
 126 F_1 , F_2 and F_3 correction factors (Table 2) that show maximum absolute differences with
 127 discrete functions lower than 7 points. These functions can be also easily implemented into
 128 software routines for SMR assessment.

129

130

131

132

133 Table 2. Asymptotical continuous functions for F_1 , F_2 and F_3 calculation, (Tomás et al.
134 2007).

| Parameter | Planar failure | Toppling failure |
|-----------|--|---|
| F_1 | $F_1 = \frac{16}{25} - \frac{3}{500} \operatorname{atan} \left(\frac{1}{10} (A - 17) \right)$ | |
| F_2 | $F_2 = \frac{9}{16} + \frac{1}{195} \operatorname{atan} \left(\frac{17}{100} B - 5 \right)$ | $F_2 = 1$ |
| F_3 | $F_3 = -30 + \frac{1}{3} \operatorname{atan} C$ | $F_3 = -13 - \frac{1}{7} \operatorname{atan} (C - 120)$ |

A is equal to the parallelism between discontinuities and slope strikes for planar and toppling failures and the angle formed between the intersection of the two discontinuities (the plunge direction) and the slope dip direction for wedge failure.
 $B = \beta_j$ or β_i
 $C = \beta_j - \beta_s$ for plane failure, $C = \beta_i - \beta_s$ for wedge failure and $C = \beta_j + \beta_s$ for toppling failure.
 β_j = joint dip angle; β_i = line of joint intersection dip angle; β_s = slope dip angle.
 Note that atan has to be expressed in degrees.

135
136 Once the SMR of a slope has been calculated, the slope can be classified within one of
137 the five different stability classes shown in Table 3. Each one of these classes is associated
138 empirically with a different failure mode. Table 3 also provides recommendations of remedial
139 measurements of a slope based on SMR depending on the stability class.

140
141 Table 3. Description of SMR classes (Romana 1985).

| Class n° | V | IV | III | II | I |
|--------------------|-------------------------|------------------------|----------------------------|-------------|-------------------|
| SMR | 0 - 20 | 21 - 40 | 41 - 60 | 61 - 80 | 81 - 100 |
| Description | Very bad | Bad | Fair | Good | Very good |
| Stability | Completely unstable | Unstable | Partially stable | Stable | Completely stable |
| Failures | Big planar or soil-like | Planar or big wedges | Some joints or many wedges | Some blocks | None |
| Support | Reexcavation | Important / corrective | Systematic | Occasional | none |

142
143 **3. DETAILED DESCRIPTION OF SMR CORRECTION FACTORS**

144 The correct and accurate determination of parameters F_1 , F_2 and F_3 is crucial for a
145 reliable calculation of the SMR index. SMR is especially sensitive to F_1 and F_2 parameters
146 (Tomás et al. 2012b), since their product ($\Psi = F_1 \times F_2$) can be considered as the percentage of
147 factor F_3 mobilized (Tomás et al. 2012a). Therefore, a special attention has to be paid in the
148 calculation of the auxiliary angular relationships. A wrong determination of some of the

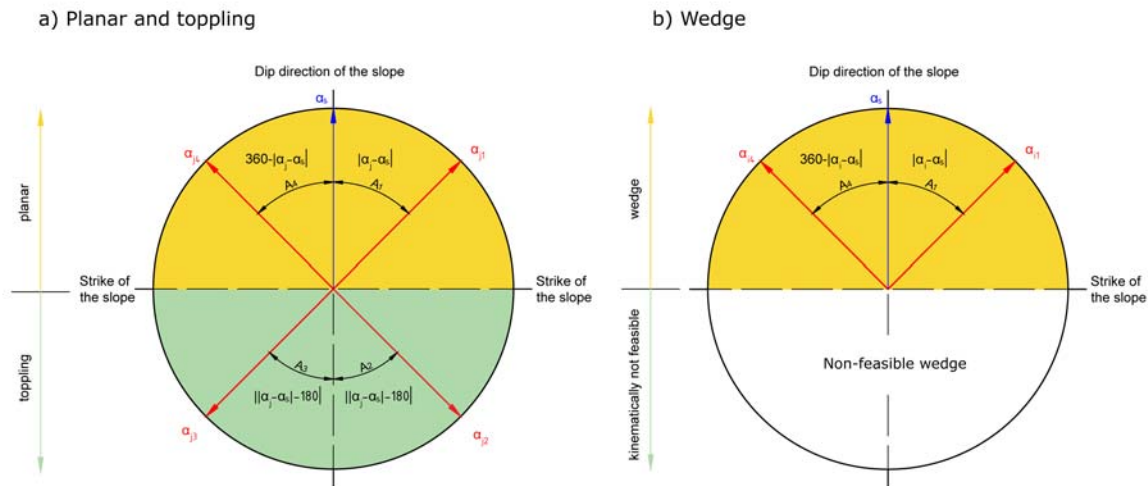
149 correction parameters can lead to a sub-estimation or an overestimation of the geomechanic
150 quality of the slope and, thus, of the evaluation of its stability.

151 The first step for a systematic definition of the parameters is the description of the involved
152 variables. To this aim, hereinafter, it is adopted that α_j and α_s are the discontinuity and slope
153 dip directions and β_j and β_s the discontinuity and slope dip angles, respectively. Three
154 auxiliary angles are used to define F_1 , F_2 and F_3 adjustment factors: A, B and C, as defined by
155 Tomás et al. (2007).

156 A refers to the parallelism between discontinuities and slope strike for planar and
157 toppling failures (Fig. 2 and Fig. 3) and the angle formed between the intersection of the two
158 discontinuities (the plunge direction) and the slope dip direction for wedge failure (Fig. 4).
159 Originally, Romana (1985) stated in a general way that the parallelism (i.e. A angle) could be
160 calculated as:

$$A = \begin{cases} |\alpha_j - \alpha_s| & \text{for planar failure} \\ |\alpha_j - \alpha_s - 180^\circ| & \text{for toppling failure} \end{cases} \quad (4)$$

161
162
163 However, these formulas are not valid for the calculus of the parallelism between the slope
164 and the discontinuity (A) in all possible relative orientations, leading to errors in its
165 calculation and therefore in the estimation of SMR. According to (4), angles higher than 90°
166 are possible, although the parallelism between the discontinuity and slope strikes has to be
167 always equal or less than 90° . This is the main source of error when calculating SMR and
168 thus, a detailed description of this parameter is required as follows. When $|\alpha_j - \alpha_s|$ is less than
169 90° planar failure is expected and A is directly equal $|\alpha_j - \alpha_s|$. Nevertheless, a mathematical
170 correction is needed in all other cases. When $|\alpha_j - \alpha_s|$ is higher than 270° planar failure is also
171 expected but A is equal to $360^\circ - |\alpha_j - \alpha_s|$. Toppling failure is expected when $|\alpha_j - \alpha_s|$ is between
172 90° and 270° , so in this case, instead of the equation $|\alpha_j - \alpha_s - 180^\circ|$ which is only valid when α_j
173 $\geq \alpha_s$, the most general equation $||\alpha_j - \alpha_s| - 180^\circ|$ should be used to the assessment of A. For
174 wedge failure, the two joints intersection line dip direction (α_i) is taken into account to study
175 the parallelism between this line and the slope dip direction. When $|\alpha_i - \alpha_s|$ is less than 90° or
176 higher than 270° a wedge failure can happen. Nevertheless, when $|\alpha_i - \alpha_s|$ is between 90° and
177 270° the wedge failure is kinematically not feasible (i.e. the wedge dips towards the slope),
178 Fig. 5.

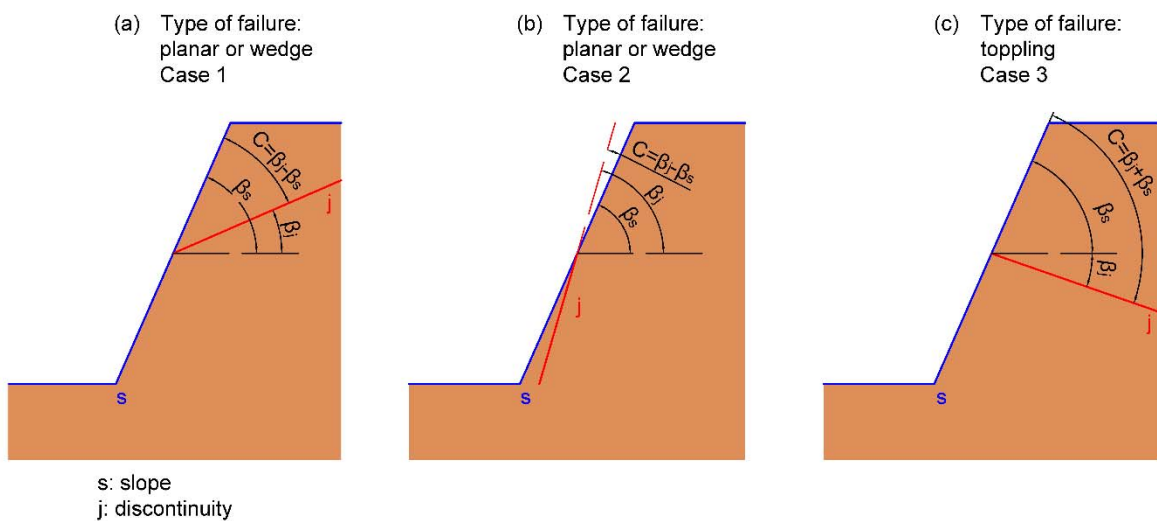


179

180 Fig. 5 – Calculation of the auxiliary angle A for a) planar and toppling failure and b) Wedge
 181 failure. The figure can be turned to make α_s perpendicular to the strike of the slope under
 182 consideration.

183 B angle is less problematic when calculated. The auxiliary angle B is the dip angle of
 184 the discontinuity or wedge, and no conversion is needed. The only caution to keep in mind
 185 when calculating the F_2 parameter is that it is always 1 for toppling failure.

186 Finally, the auxiliary angle C is the relation between discontinuity dip angle and slope
 187 dip angle. Its calculation is also quite simple and is shown in Fig. 6 . For planar and wedge
 188 failures C is equal to $\beta_j - \beta_s$ and $\beta_t - \beta_s$, respectively, and can adopt positive (Fig. 6 - b) or
 189 negative (Fig. 6 - a) values. For toppling, C is calculated as $\beta_j + \beta_s$ (Fig. 6 - c). Therefore,
 190 the identification of the failure mode compatible with each discontinuity is required before the
 191 calculation of this parameter.



192

193 Fig. 6 – Calculation of the auxiliary angle C. (a) and (b) show two possible cases of planar
194 failure; (c) shows a toppling.

195 Table 4 summarizes the formulas used for the calculation of A, B and C angular
196 relationships for the determination of F_1 , F_2 and F_3 parameters, respectively, using the dip and
197 dip direction of the slope and the discontinuities affecting the slope.

198 Table 4. Summary of the formulas used for the calculation of A, B and C angular
199 relationships.

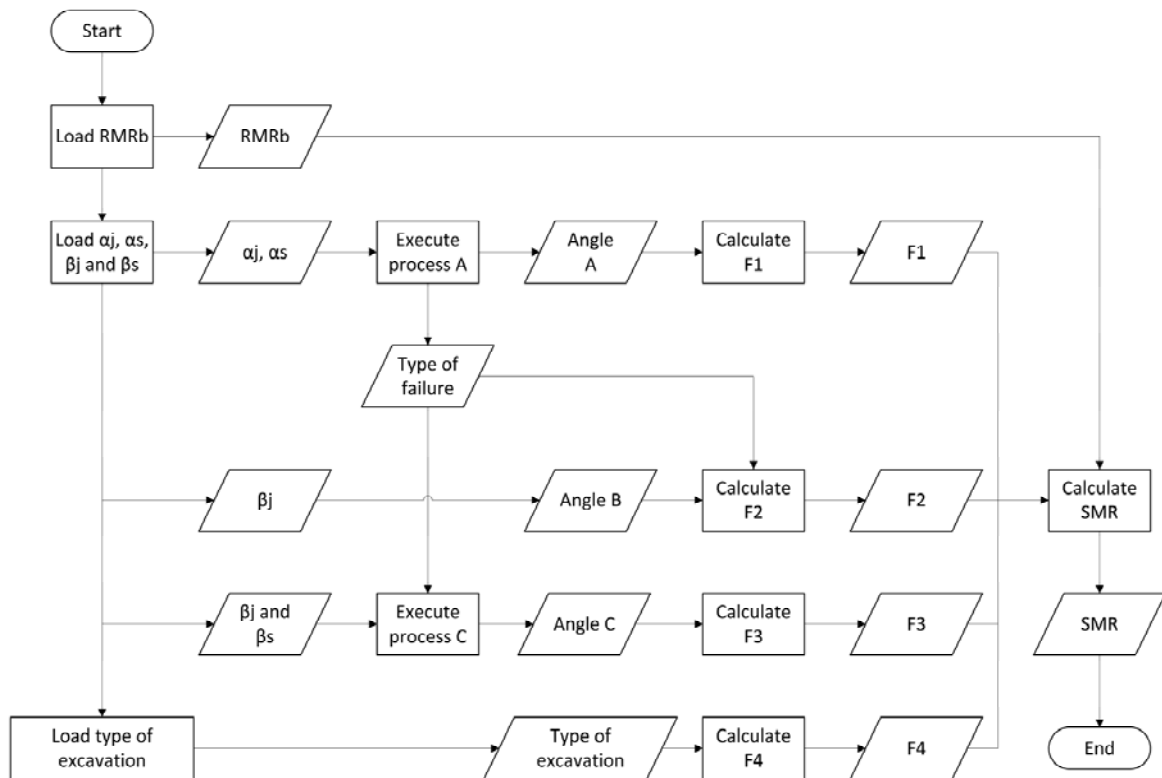
| Failure mode | Angular relationship | Calculation of A | Calculation of B | Calculation of C |
|--------------|--|---|------------------|-------------------------|
| Planar | $ \alpha_j - \alpha_s < 90^\circ$ | $A = \alpha_j - \alpha_s $ | $B = \beta_j$ | $C = \beta_j - \beta_s$ |
| | $ \alpha_j - \alpha_s > 90^\circ$ | $A = 360^\circ - \alpha_j - \alpha_s $ | $B = \beta_j$ | $C = \beta_j - \beta_s$ |
| Wedge | $ \alpha_i - \alpha_s < 90^\circ$ | $A = \alpha_i - \alpha_s $ | $B = \beta_i$ | $C = \beta_i - \beta_s$ |
| | $ \alpha_i - \alpha_s > 90^\circ$ | $A = 360^\circ - \alpha_i - \alpha_s $ | $B = \beta_i$ | $C = \beta_i - \beta_s$ |
| Toppling | $90^\circ < \alpha_j - \alpha_s < 270^\circ$ | $A = \alpha_j - \alpha_s - 180^\circ $ | Not necessary | $C = \beta_j + \beta_s$ |

200

201

202 4. OPEN-SOURCE SOFTWARE DESCRIPTION

203 An open source software has been developed for an automatic and accurate calculation
204 of the angular relationships and parameters involved in the calculation of SMR
205 (<https://personal.ua.es/en/ariquelme/smrtool.html>). This software will help engineers and
206 geologists with a graphical representation of the geometry data used as input for the SMR
207 calculation and guiding them in the whole process. The process followed by the software for
208 the SMR assessment can be seen in Fig. 7.



209

210 Fig. 7 – Flowchart for the SMR calculation.

211

212 The pseudocodes of the processes A, F₁, F₂, C and F₃ (Fig. 7) are described in the Algorithms

213 1 to 5 (Fig. 8 to 12). It is worth noting that when a wedge instability is being calculated, the

214 software equals $\alpha_i = \alpha_j$, and $\beta_i = \beta_j$ using the same algorithm as for planar failure.

215

procedure A

Input: α_s, α_j

Output: A, type-of-failure

$A \leftarrow |\alpha_s - \alpha_j|$

type-of-failure \leftarrow planar-wedge

if $A > 90^\circ$ and $A < 270^\circ$ **then**

 type-of-failure \leftarrow toppling

if $A > 180^\circ$ **then**

$A \leftarrow A - 180^\circ$

else

$A \leftarrow 180^\circ - A$

if $A \geq 270^\circ$ and $A \leq 360^\circ$ **then**

$A \leftarrow 360^\circ - A$

216

217 Fig. 8 – Algorithm 1. Pseudocode for the process A.

218

219

220

221

```

procedure  $F_1$ 
  Input:  $\alpha_s, \alpha_j, A$ 
  Output:  $F_1$ 
  if  $A > 30^\circ$  then
     $F_1 \leftarrow 0.15$ 
  if  $A \geq 20^\circ$  and  $A < 30^\circ$  then
     $F_1 \leftarrow 0.4$ 
  if  $A \geq 5^\circ$  and  $A < 10^\circ$  then
     $F_1 \leftarrow 0.85$ 
  if  $A < 5^\circ$  then
     $F_1 \leftarrow 1$ 

```

222

223 Fig. 9 - Algorithm 2 Pseudocode for the process F_1 .

224

```

procedure  $F_2$ 
  Input: type-of-failure,  $\beta_j$ 
  Output:  $F_2$ 
  if type-of-failure = toppling then
     $F_2 \leftarrow 1$ 
  else
    if  $\beta_j \leq 20^\circ$  then
       $F_2 \leftarrow 0.15$ 
    if  $\beta_j > 20^\circ$  and  $\beta_j \leq 30^\circ$  then
       $F_2 \leftarrow 0.4$ 
    if  $\beta_j > 30^\circ$  and  $\beta_j \leq 35^\circ$  then
       $F_2 \leftarrow 0.7$ 
    if  $\beta_j > 35^\circ$  and  $\beta_j \leq 45^\circ$  then
       $F_2 \leftarrow 0.85$ 
    if  $\beta_j > 45^\circ$  then
       $F_2 \leftarrow 1$ 

```

225

226 Fig. 10 - Algorithm 3 Pseudocode for the process F_2 .

227

```

procedure C
  Input:  $\beta_j, \beta_s$ , type-of-failure
  Output: C
  if type-of-failure = toppling then
     $C \leftarrow \beta_s + \beta_j$ 
  else
     $C \leftarrow \beta_j - \beta_s$ 

```

228

229 Fig. 11 - Algorithm 4 Pseudocode for the process C.

230

```
procedure  $F_3$ 
Input:  $C$ , type-of-failure
Output:  $F_3$ 
if type-of-failure = toppling then
  if  $C < 110^\circ$  then
     $F_3 \leftarrow 0$ 
  if  $C \geq 110^\circ$  and  $C < 120^\circ$  then
     $F_3 \leftarrow -6$ 
  if  $C \geq 120^\circ$  then
     $F_3 \leftarrow -25$ 
else
  if  $C > 10^\circ$  then
     $F_3 \leftarrow 0$ 
  if  $C > 0^\circ$  and  $C \leq 10^\circ$  then
     $F_3 \leftarrow -6$ 
  if  $C = 0^\circ$  then
     $F_3 \leftarrow -25$ 
  if  $C \geq -10^\circ$  and  $C < 0^\circ$  then
     $F_3 \leftarrow -50$ 
  if  $C \leq -10^\circ$  then
     $F_3 \leftarrow -60$ 
```

231

232 Fig. 12 - Algorithm 5 Pseudocode for the process F_3 .

233

234 A compact graphical user interface has been designed, allowing the user to check the
235 inputs and outputs in the same window. This graphical user interface is shown in Fig. 13 . The
236 *Input data* panel can be seen on the top left and the top centre of this figure. As input data, the
237 user must introduce the slope geometry (dip direction and dip), the slope excavation method,
238 which is chosen from a list, the discontinuity geometry (dip direction and dip) and the Rock
239 Mass Rating of the set of discontinuities for which the SMR wants to be calculated. In this
240 case, in which the analysis is being done for an individual set of discontinuities, the user must
241 choose the type of element analyzed between plane or wedge. If the user wants to run the
242 analysis not for one individual set of discontinuities but for all sets of discontinuities within
243 the rock mass, *Planes and Wedges* panel should be used. This panel is in the centre of the
244 upper half of the graphical user interface. Geometry and RMR for each discontinuity or set of
245 discontinuities to be considered have to be introduced here. In this case, it is not necessary to
246 select the type of element being analyzed, as after clicking the button “Calculate wedges”, the
247 software will calculate all the possible wedges from the intersecting plane discontinuities and
248 analyze if the failure is kinetically possible. When the wedge is kinetically non-possible a
249 value of 0 is shown in the possibility section of the *Planes and Wedges* panel, and the SMR
250 for this wedge is shown as equal to 100, meaning that there are no stability problems for this
251 wedge.

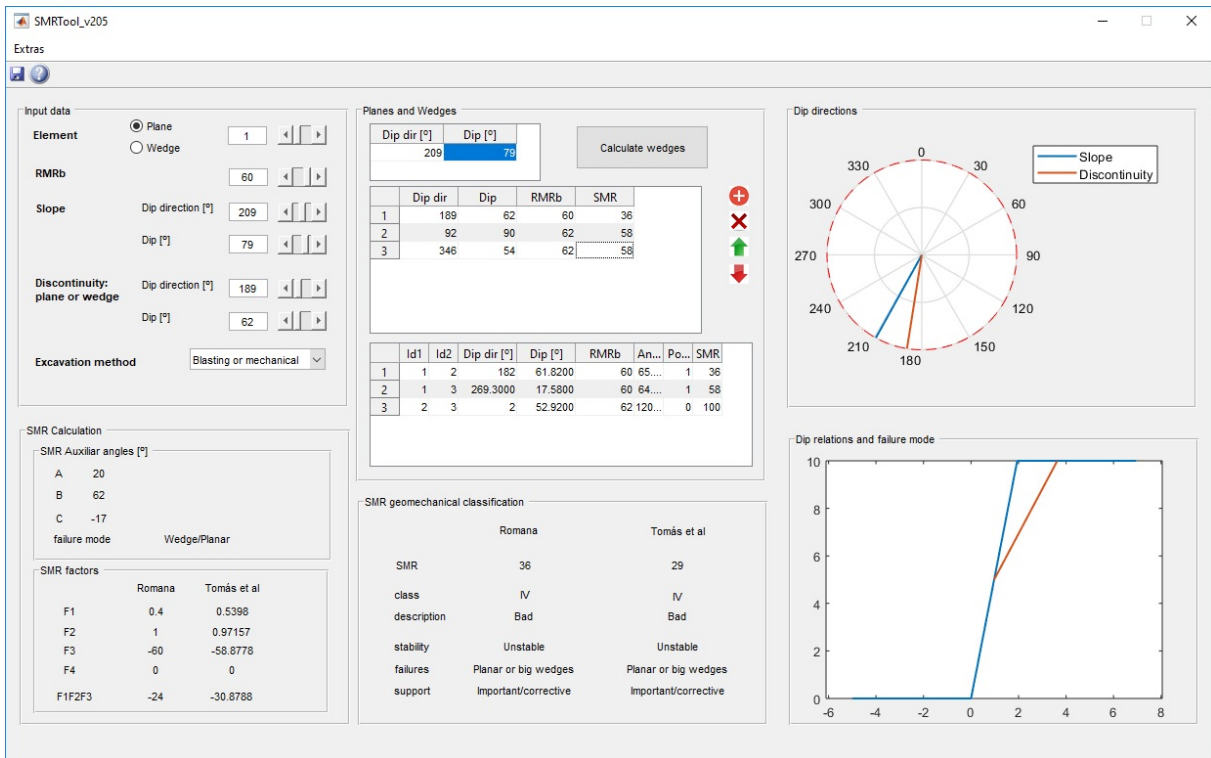
252 Based on the dip and dip direction of the slope and discontinuities (Clar's notation),
253 the possible slope failure type is calculated by the software. As said in the previous section,
254 the formulae to be used to assess the parameters F_1 , F_2 and F_3 depends on the type of failure
255 considered (i.e. plane, wedge or toppling) and considers all possible geometrical situations
256 illustrated in Fig. 5 and Fig. 6. Therefore, the automatic assessment by the software avoids
257 mistakes in this step.

258 All the intermediate calculations are shown on the SMR Calculations panel. The upper
259 half of this panel shows the SMR auxiliary angles A, B, and C previously described. The
260 parameters F_1 , F_2 , F_3 and F_4 calculated according to Romana (1985) and Tomás et al. (2007)
261 are presented on the lower half panel, allowing users to compare the results obtained between
262 these two methods.

263 The SMR result is shown on the SMR Geomechanics Classification panel, which is in
264 the centre of the lower half of the graphical user interface. In addition to the SMR numerical
265 result, the stability classification of the slope, the description, the stability, the expected type
266 of failure and the remedial measurement recommended according to Romana (1993) are also
267 shown on this panel. Therefore, this is the results main panel, showing all the necessary data
268 to analyze the slope stability.

269 Finally, two graphical representations of the relative orientation between slope and
270 discontinuities are depicted at the right side of the interface, helping users to understand the
271 expected type of failure. The figure on the upper right-hand side shows a top view of the
272 angle between the slope and the discontinuity dip directions. Plane or wedge failure, but no
273 toppling, will be expected when the angle between these two vectors is less than 90° (acute
274 angle). On the contrary, only toppling can be expected when the angle is obtuse. The figure on
275 the lower right-hand side shows a cross section of the slope in which the discontinuity has
276 been depicted. This figure clarifies the type of failure expected (plane, wedge or toppling)
277 according to the slope and discontinuity geometry. These two figures have clarifying purpose
278 as they make clear the importance of related properties of the slope geometry and the
279 direction and dip of the discontinuities within the stability calculations, avoiding mistakes
280 involving the relative orientation between discontinuities and slope. It is worth noting that this
281 kind of miscalculation is the most common when applying SMR.

282



283
284 Fig. 13 – Graphical user interface of the SMRTool software.

285
286 **5. CASE STUDY**

287 A case study of an 18 m high slope composed of Jurassic slightly weathered limestone
288 (Martín and Campos 1974) with a strong structural control is presented in this section in order
289 to illustrate the applicability of the developed software and the calculation of the angular
290 relationships and correction parameters. A general view of the slope of the example is shown
291 in Fig. 14 . All the necessary geomechanical data obtained during the field works and in the
292 previous calculations for SMR assessment of the slope are summarized in Table 5. In this
293 case, three sets of discontinuities were recognized in the slope: DS1 to DS3.

294
295 Table 5. Data obtained in the field and previous calculations for SMR assessment.

| Discontinuity set | Dip Direction (°) | Dip (°) | RMR _b |
|---------------------------------------|-------------------|---------|------------------|
| Slope Mechanical excavation | 209 | 79 | -- |
| DS1 | 189 | 62 | 60 |
| DS2 | 92 | 90 | 62 |
| DS3 | 346 | 54 | 62 |

297
298
299
300
301
302
303
304
305
306
307
308

Fig. 13 shows the SMRTool graphical user interface using the input data of Table 5. These input parameters can be seen in the top centre panel in which dip direction and dip of the slope are first shown. The dip direction and dip of the three sets of discontinuities are included below. The mechanical excavation method is introduced in the top left panel, where the data of plane 1 (discontinuity set 1) can also be seen. Once all the data have been introduced, the SMR values for each discontinuity set is shown in the last column of the top centre panel. SMR values of 36, 58 and 58 are obtained for DS1, DS2 and DS3, respectively. The software runs the wedges analysis by clicking the *Calculate wedges* button in the top centre panel. After doing this, the SMR values for the possible wedges are shown in the centre of the graphical user interface.



309
310
311
312

Fig. 14 – View of the slope of the example where three discontinuity sets can be distinguished.

313
314
315
316

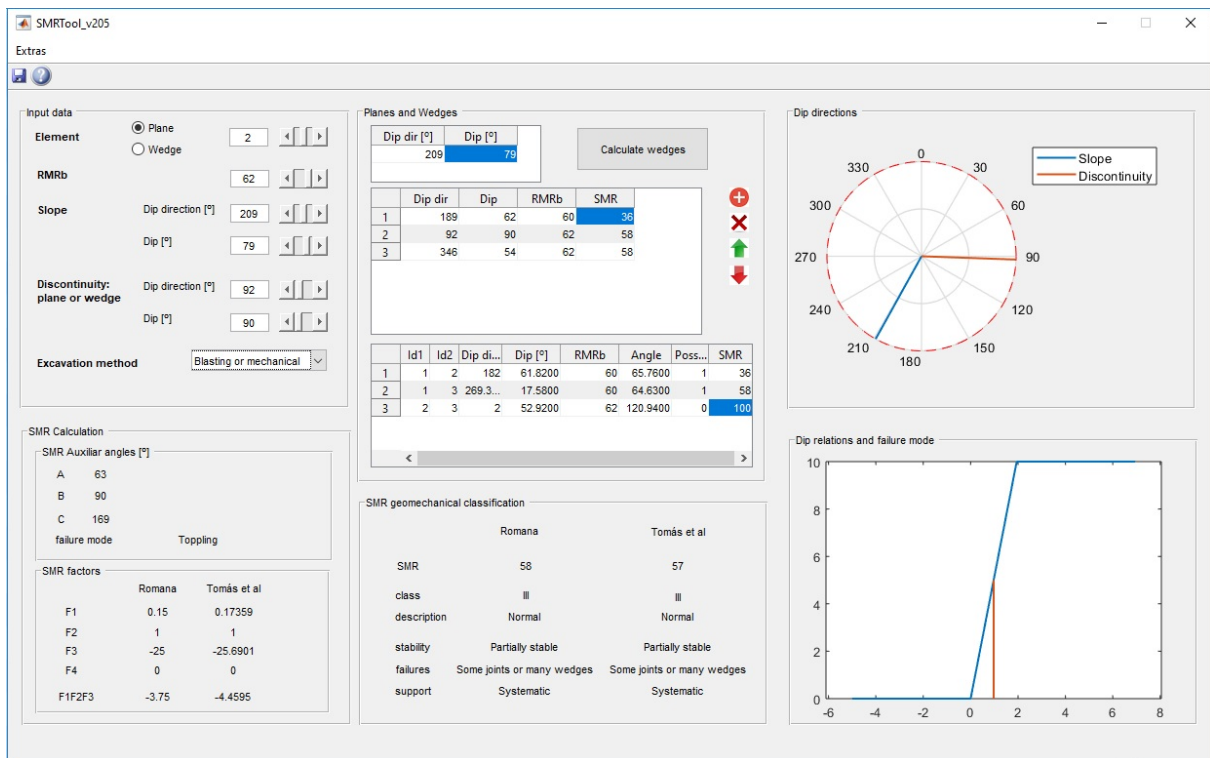
In order to better understand the calculation process, the value of the auxiliary angles A, B and C are shown in the SMR panel, where the likely failure mode is outlined. A, B and C angles of 20°, 62° and -17° are obtained for plane 1 (DS1), being wedge or planar the possible failure mode. The SMR factors are shown on the lower half of the SMR panel, where

317 it can be seen the difference between these factors calculated according to the discrete values
318 proposed by Romana (1993) and according to the continuous functions proposed by Tomás et
319 al. (2007). The first factor, for example, equals 0.4 when calculated by Romana (1993) and
320 0.5398 when calculated by Tomás et al. (2007). This example illustrates the benefit of using
321 the continuous functions for the factor assessment, especially when the parameters, are near
322 the borderline between two different ratings. In this case, the absolute value of the difference
323 between joint dip direction and slope dip direction for factor 1 equals 20° . Therefore F_1 can be
324 rated as 0.4 or 0.7 according to Table 1 (Romana 1993), whilst the continuous functions do
325 not exhibit this issue.

326 The SMR numerical result for plane 1 (DS1) is shown in the SMR Geomechanics
327 Classification panel, being equal to 36 when the factors are calculated according to the
328 original discrete functions (Romana 1993) and equal to 29 when are calculated using the
329 continuous functions (Tomás et al. 2007). Despite the difference of the SMR value obtained
330 by these two methods for this example, for both cases, the stability classification is IV. Being
331 the description “bad” and unstable, with planar or big wedges failures expected, and important
332 corrective measures needed. Finally, the dip direction graphical representation shows the
333 alignment between slope and discontinuity dip direction, needed for factor 1 assessment. The
334 dip directions and failure mode representation let the user understand why a planar failure
335 mode is expected for plane 1 (DS1) (see the failure modes presented in Fig. 1).

336 We can change the data shown on the graphical user interface by clicking on the
337 number of the plane shown on the top left panel (i.e. the input data panel). If we set the plane
338 number 2 (DS2), all the data, results and plots shown will correspond to this plane, Fig. 15 .
339 In this case, toppling failure is expected, being all the calculations done (auxiliary angles, etc.)
340 according to this type of failure. Looking at the dip directions (upper right plot) and failure
341 mode representation (lower right plot) it can be seen that the slope and the discontinuity set
342 are dipping in opposite directions. Therefore, it is easy to understand why toppling is the
343 expected type of failure. The calculated SMR value for DS2 is equal to 58 and 57 calculated
344 by Romana (1993) and Tomás et al. (2007), respectively. Dip direction representation, where
345 no alignment between discontinuity and slope direction are seen, explains these SMR values
346 higher than those calculated for plane 1. For both SMR values (i.e. discrete and continuous),
347 the stability classification is III, described as “normal”, being partially stable with some joints
348 or many wedges expected, needing systematic corrective measures. It is noteworthy that the
349 results of the auxiliary angle A for DS2 are different when calculated according to the general

350 equation $||\alpha_j - \alpha_s| - 180^\circ|$, included in the detailed description of angular relationships of Table
 351 4, and using the original equation $|\alpha_j - \alpha_s - 180^\circ|$ from Romana (1993). In this particular case,
 352 the parallelism (A) is equal to 63° when it is calculated according to the proposed equation,
 353 and this is the value shown by the SMRTool software, Fig. 15 and Table 6. However, a value
 354 of 297° is obtained by the use of the original general equation published by Romana (1993).
 355 By coincidence, the value of F_1 is the same for both angles (0.15). Nevertheless, if the slope
 356 dip direction were 60° smaller, F_1 would be equal to 1 calculated with the proposed equation
 357 and 0.15 calculated with the equation from Romana (1993). This miscalculation would lead to
 358 a very different stability assessment. In fact, the calculation made using the relationships
 359 listed in Table 5 would be on the safe of security in comparison with those made using the
 360 general expression proposed by Romana (1993).
 361



362
 363 Fig. 15 – Graphical User Interface for plane 2.

364
 365 The complete results of this case study are shown in Table 6. All the instabilities
 366 possible combinations between slope and the three discontinuity sets are shown in this table.
 367 One planar failure, two toppling and five wedges were analyzed by the software. The use of
 368 the SMRTool allows the user to obtain all this data automatically, making more efficient and
 369 quicker the calculation, and avoiding mistakes involving the relative orientation between

370 discontinuities and slope. For this case study, the discontinuity set 1 has the worst influence
 371 on the stability of the slope. An SMR value of 36 has been obtained using the discrete
 372 functions (Romana 1993) and of 29 using the continuous functions (Tomás et al. 2007). The
 373 last wedge in Table 6 is not kinematically feasible, as the dip of the wedge is towards the
 374 slope, therefore the software shows a value of 0 in the possibility button of the *Planes and*
 375 *Wedges* panel, and the SMR for this wedge is shown as equal to 100. It means that there are
 376 no stability problems for the considered wedge.

377

378 Table 6. Results obtained using SMRTool for the case study for discrete functions
 379 when calculated by Romana (Romana 1993) and for continuous functions when calculated by
 380 Tomás et al. (Tomás et al. 2007).

| Type of failure | Discontinuity set involved | Auxiliary angles (°) | | | SMR factors | | | | | | | | SMR value | |
|-----------------|----------------------------|----------------------|-------|--------|--------------------|------|-----|----|----------------------|---------|----------|----|--------------------|----------------------|
| | | A | B | C | Discrete functions | | | | Continuous functions | | | | Discrete functions | Continuous functions |
| | | | | | F1 | F2 | F3 | F4 | F1 | F2 | F3 | F4 | | |
| Planar | DS 1 | 20 | 62 | -17 | 0.4 | 1 | -60 | 0 | 0.5398 | 0.97157 | -58.8778 | 0 | 36 | 29 |
| Toppling | DS 2 | 63 | 90 | 169 | 0.15 | 1 | -25 | 0 | 0.17359 | 1 | -25.6901 | 0 | 58 | 57 |
| Toppling | DS 3 | 43 | 54 | 133 | 0.15 | 1 | -25 | 0 | 0.22623 | 1 | -25.2288 | 0 | 58 | 56 |
| Wedge | DS 1 – DS2 | 27 | 61.82 | -17.18 | 0.4 | 1 | -60 | 0 | 0.37 | 0.97128 | -58.8896 | 0 | 36 | 38 |
| Wedge | DS 1 – DS3 | 60.3 | 17.58 | -61.42 | 0.15 | 0.15 | -60 | 0 | 0.17803 | 0.23653 | -59.6891 | 0 | 58 | 57 |
| Wedge | DS 2 – DS3 | 27 | 52.92 | 131.9 | Non-feasible wedge | | | | | | | | 100 | 100 |

381

382

383 6. CONCLUSIONS

384 Slope Mass Rating (SMR) is worldwide used to perform a preliminary assessment of
 385 rock slopes stability for different purposes such as civil or mining engineering. Nevertheless,
 386 often some miscalculations are made when professionally and scientifically used. Nearly all
 387 these mistakes involve the relative orientation between the slope and the discontinuities.
 388 Therefore, a detailed description of the geometrical parameters A, B and C involved in the
 389 calculation of SMR as never before done has been included in this paper. Furthermore, a
 390 Matlab-based open-source software to avoid the above-mentioned mistakes as well as to make
 391 more efficient and quicker the calculation of SMR has been programmed. The code of this
 392 Matlab-based software is freely downloadable online for analysis of rock slope stability and
 393 the algorithms are presented in this paper.

394

395 **7. ACKNOWLEDGEMENTS**

396 This work has been supported by the University of Alicante under the projects
397 GRE14-04 and GRE17-11, and the Spanish Ministry of Economy and Competitiveness
398 (MINECO), the State Agency of Research (AEI) and the European Funds for Regional
399 Development (FEDER) under projects TEC2017-85244-C2-1-P and TIN2014-55413-C2-2-P,
400 and the Spanish Ministry of Education, Culture and Sport under project PRX17/00439 and
401 CAS17/00392.

402

403 **8. REFERENCES**

404 Bar N, Barton N (2017) The Q-Slope Method for Rock Slope Engineering. *Rock Mech Rock*
405 *Eng* 50:3307–3322. doi: 10.1007/s00603-017-1305-0

406 Barton N, Bar N (2015) Introducing the Q-slope method and its intended use within civil and
407 mining engineering projects. In: W S, A K (eds) *Future development of rock mechanics;*
408 *Proceedings of the ISRM regional symposium, Eurock 2015 and 64th geomechanics*
409 *colloquium*. Salzburg, pp 157–162

410 Bieniawski ZT (1976) Rock mass classification in rock engineering. In: Bieniawski ZT (ed)
411 *Proceeding of the Symposium Exploration for Rock Engineering*. Johannesburg, pp 97–
412 106

413 Bieniawski ZT (1989) *Engineering Rock Mass Classification: a complete manual for*
414 *engineers and geologists in mining, civil, and petroleum engineering*. Wiley, Chichester
415 251

416 Hack R, Price D, Rengers NA (1998) A new approach to rock slope stability - a probability
417 classification (SSPC). *B Eng Geol Environ* 62:167–184

418 Hoek E, Bray JW (1981) *Rock Slope Engineering*. The Institution of Mining and Metallurgy,
419 London

420 Hudson JA, Harrison JP (1997) *Engineering Rock Mechanics: an introduction to the*
421 *principles*. Amsterdam

422 Lindsay P, Campbell RN, Fergusson DA, et al (2001) Slope stability probability
423 classification. *Int J Coal Geol* 45:127–145

424 Martín P, Campos C (1974) *Mapa Geológico de España, hoja de Sagunto*. Ministerio de
425 *Industria*

- 426 Robertson AM (1988) Estimating weak rock strength. In: Proceedings of the SME Annual
427 meeting, Society of Mining Engineering. Phoenix, pp 1–5
- 428 Romana M (1993) SMR classification. In: Proceedings of the 7th ISRM International
429 Congress on Rock Mechanics. Rotterdam: A A Balkema, Aachen, pp 955–960
- 430 Romana M (1985) New adjustment ratings for application of Bieniawski classification to
431 slopes. In: Mechanics IS of R (ed) Proceedings of the International Symposium on the
432 Role of Rock Mechanics in Excavations for Mining and Civil Works. Zacatecas, pp 49–
433 53
- 434 Romana M, Tomas R, Seron JB (2015) Slope Mass Rating (SMR) Geomechanics
435 Classification: Thirty Years Review. In: ISRM Congress 2015 Proceedings -
436 International Symposium on Rock Mechanics. Quebec, Canada, p 10
- 437 Shuk T (1994) Key elements and applications of the natural slope methodology (NSM) with
438 some emphasis on slope stability aspects. In: ISRM (ed) Proceedings of the 4th South
439 American Congress on Rock Mechanics 2. Balkema, Rotterdam, pp 955–960
- 440 Singh B, Göel RK (1999) Rock Mass Classification. A practical Approach in Civil
441 Engineering. Amsterdam
- 442 Tomás R, Cuenca A, Cano M, García-Barba J (2012a) A graphical approach for slope mass
443 rating (SMR). *Eng Geol* 124:67–76. doi: 10.1016/J.ENGGEOL.2011.10.004
- 444 Tomás R, Delgado J, Serón JB (2007) Modification of Slope Mass Rating (SMR) by
445 continuous functions. *Int J Rock Mech Min Sci* 44:1062–1069
- 446 Tomás R, Romana M, Serón JB (2016) Revisión del estado actual de la clasificación
447 geomecánica Slope Mass Rating (SMR). In: 10° Simposio Nacional ingeniería
448 Geotécnica. La Coruña, pp 19–21
- 449 Tomás R, Valdes-Abellan J, Tenza-Abril AJ, Cano M (2012b) New insight into the slope
450 mass rating geomechanical classification through four-dimensional visualization. *Int J*
451 *Rock Mech Min Sci* 53:64–69. doi: 10.1016/J.IJRMMS.2012.04.002
- 452 Zheng J, Zhao Y, Lü Q, et al (2016) A discussion on the adjustment parameters of the Slope
453 Mass Rating (SMR) system for rock slopes. *Eng Geol* 206:42–49. doi:
454 10.1016/J.ENGGEOL.2016.03.007
- 455